

Short Communication

## Preparation of SnO<sub>2</sub> Nanoparticle and Performance as Lithium-ion Battery Anode

Lili Feng<sup>1,\*</sup>, Zhewen Xuan<sup>1</sup>, Siping Ji<sup>1</sup>, Weiru Min<sup>1</sup>, Hongbo Zhao<sup>1</sup>, Hui Gao<sup>2,\*</sup>

<sup>1</sup> Engineering Research Center of Biopolymer Functional Materials of Yunnan, Yunnan Minzu University, Kunming 650500, China

<sup>2</sup> School of Pharmacy, Yunnan University of Traditional Chinese Medicine, Kunming 650550, China

\*E-mail: [lilylian2003@163.com](mailto:lilylian2003@163.com) (Lili Feng) or [gaohui\\_em@126.com](mailto:gaohui_em@126.com) (Hui Gao)

Received: 17 November 2014 / Accepted: 8 December 2014 / Published: 19 January 2015

---

Herein we report that SnO<sub>2</sub> nanoparticle is successfully prepared by the hydrolysis of SnCl<sub>2</sub> as sodium dodecyl benzene sulfonate (SDBS) is used as the surfactant. The structures and electrochemical performances are characterized by scanning electron microscope (SEM), X-ray diffraction (XRD), galvanostatic cell cycling and electrochemical impedance spectroscopy (EIS). The morphology of the SnO<sub>2</sub> nanoparticle is spherical. The SnO<sub>2</sub> nanoparticle is cassiterite type which belongs to tetragonal crystal system with rutile structure. The results of galvanostatic cell cycling performances show that the SnO<sub>2</sub> nanoparticle has high discharge specific capacity, but with relative low cycling stability. The sample calcinated for 9h has higher discharge specific capacity and lower electrochemical impedance.

---

**Keywords:** Nanoparticles; SnO<sub>2</sub>; Hydrolysis method; Lithium-ion batteries; Anode materials

### 1. INTRODUCTION

In recent years, as the development of the economy, the requirement and consumption of energy is increasing. New green high-performance secondary power as a clean and efficient energy storage and conversion device, plays an important role in new energy exploitation and environmental protection, and has become one of the areas of worldwide competing for the development. Lithium-ion battery is widely used in mobile electronic devices, electric vehicles, alternate energy storage, smart electricity grid system and other fields, due to its high voltage, high energy, light weight, small size, low internal resistance, low self-discharge, long cycle life, no memory effect. Now to develop advanced rechargeable lithium-ion battery, new electrode materials are requires.

As early as 2000, Tarascon's research group reported that electrodes made of nanoparticles of transition-metal oxides (MO, where M is Co, Ni, Sn or Fe) demonstrated electrochemical capacities of more than 700 mAh g<sup>-1</sup> (this value was approximately twice of the theoretical capacity of the carbon material[1]) and high recharging rates. Therefore, many efforts have so far been made to preparing micro or nano metal oxides with various morphologies as well as various structures, especially for the design, synthesis and applications of SnO<sub>2</sub> nanostructures[2, 3]. SnO<sub>2</sub> possess high theoretically gravimetric lithium storage capacity of about 710 mAh g<sup>-1</sup> and low potential of lithium ion intercalation, so it is regarded as one of the most promising candidates for anode materials[4-11]. For an example, Xie group[12] prepared SnO<sub>2</sub> hollow sphere and rod materials by the oxidation-crystallization method of amorphous colloids. The measured capacities of SnO<sub>2</sub> hollow sphere and rod electrodes were 698 and 470 mAh g<sup>-1</sup>, respectively. And they were higher than that of a solid SnO<sub>2</sub> nanoparticles electrode (650 mAhg<sup>-1</sup>). Han et al.[13] had synthesized hollow SnO<sub>2</sub> microspheres by heat treatment of tin chloride/RF gel composite. When the SnO<sub>2</sub> microspheres were employed as a lithium-ion battery anode, they exhibited extraordinarily high discharge capacities and higher coulombic efficiency. Wang et al.[14] had prepared SnO<sub>2</sub> nanosheets which had a high discharge capacity of 559 mAh g<sup>-1</sup> after 20 cycles with good retention of 57%.

The above examples suggested that if single SnO<sub>2</sub> was used as an active material, it should be in a nanometer-sized frame to shorten the pathway lengths of the lithium ion or should possess interior hollow spaces to accommodate large volume change. In the present work, to improve the electrochemical performances of SnO<sub>2</sub> anode materials, SnO<sub>2</sub> nanoparticle was prepared. Here SnO<sub>2</sub> nanoparticle was prepared by the hydrolysis of SnCl<sub>2</sub>, and then by calcination in a muffle furnace at 700 °C for 7~9 h in air atmosphere.

## 2. EXPERIMENTAL SECTION

### 2.1 Synthesis and Characterization of SnO<sub>2</sub> Nanoparticle

All reagents purchased from the Shanghai Chemical Company were of analytical grade, and used without further purification. To prepare SnO<sub>2</sub> nanoparticle, 2.2565g SnSO<sub>4</sub> and 3.4835g sodium dodecyl benzenesulfonate (SDBS) were dissolved in 100 mL of distilled water and stirred for 9 h at room temperature. After the reaction was completed, the white precipitation were washed and harvested with centrifugation-redispersion cycles for several times with distilled water, and dried at 80 °C for 12 h. Then the white precipitation was grinded for 20 minutes, and the SnO<sub>2</sub> nanoparticle were obtained by calcined in a muffle furnace at 700 °C for 7 h or 9 h in air atmosphere.

The morphological investigations of SEM images were taken on a field emission scanning electron microscope (QUANTA-200 America FEI Company), The crystallographic structures of the products were determined with XRD which were recorded on a Rigaku D/max-2200/PC with Cu target at a scanning rate of 7°/min with 2θ ranging from 20 to 70°.

## 2.2 Electrochemical Studies of SnO<sub>2</sub> Nanoparticle

Electrochemical performances of the samples were measured using CR2025 coin-type cells assembled in a dry argon filled glove box. To fabricate the working electrode, a slurry consisting of 60 wt.% active materials, 10 wt.% acetylene black, and 30 wt.% poly-vinylidene fluoride (PVDF) dissolved in N-methyl pyrrolidinone was casted on a copper foil, drying at 80 °C under vacuum for 5 h. Lithium sheets were served as counter and reference electrodes, while a Celgard 2320 membrane was employed as a separator. The electrolyte was a solution of 1 M LiPF<sub>6</sub> in ethylene carbonate (EC)-1,2-dimethyl carbonate (DMC) (1:1 in volume). Galvanostatical charge-discharge experiments were performed by Land electric test system CT2001A (Wuhan Jinnuo Electronics Co., Ltd.) at a current density of 0.2 C between 0.01 and 3.00 V (versus Li/Li<sup>+</sup>). Electrochemical impedance spectroscopy (EIS) measurements were performed on an electrochemical workstation (CHI604D, Chenhua, Shanghai), and the frequency ranged from 0.1 Hz to 100 KHz with an applied AC signal amplitude of 5 mV.

## 3. RESULTS AND DISCUSSION

### 3.1 Structure and Morphology

The SEM image of the as-prepared SnO<sub>2</sub> nanoparticle is displayed in Fig. 1. As shown the as-prepared SnO<sub>2</sub> nanoparticle is spheric morphology with about 45 nm in diameter. Fig. 1 suggests that the SnO<sub>2</sub> nanoparticles tend to agglomerate into larger particles.

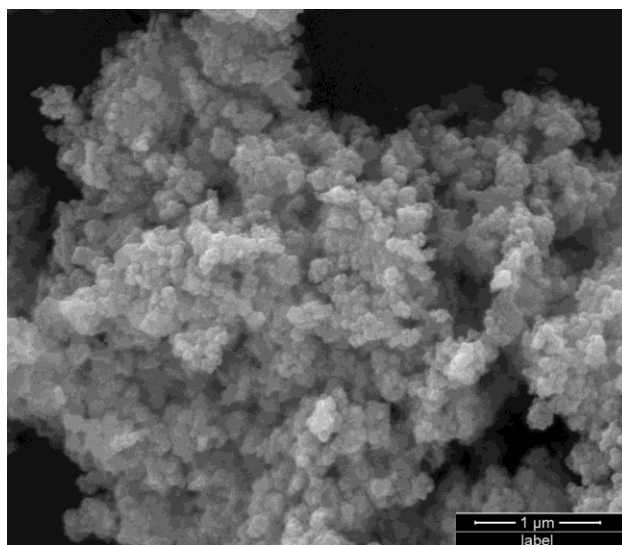


**Figure 1.** SEM image of the as-prepared SnO<sub>2</sub> nanoparticle. The scale bar is 1 μm.

The XRD patterns of the as-prepared SnO<sub>2</sub> nanoparticle are shown in Fig. 2. The two samples have similar crystallographic structure. The diffraction peaks appeared at  $2\theta=26.6^\circ$ ,  $33.9^\circ$ ,  $38^\circ$ ,  $51.9^\circ$ ,

55.0° match well with the diffraction peaks of (110), (101), (200), (211), and (220) crystal planes of SnO<sub>2</sub> standard data (JCPDS card PDF file No. 41–1445). As shown in Fig. 2, the SnO<sub>2</sub> samples are both cassiterite type which belongs to tetragonal crystal system with rutile structure.

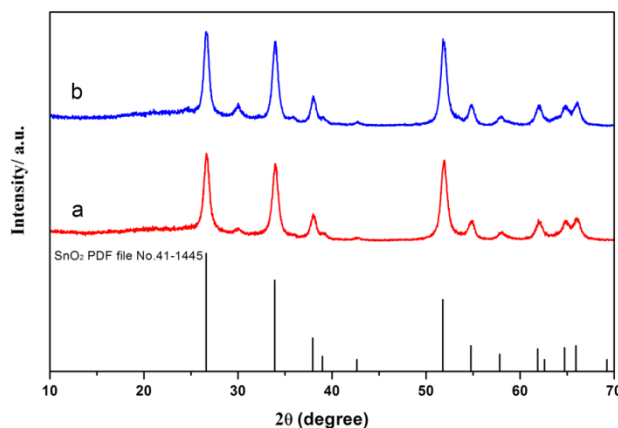


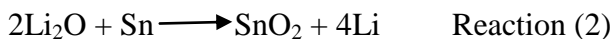
**Figure 2.** The XRD patterns of the as-prepared SnO<sub>2</sub> nanoparticle. (a) sample calcinated for 7h , (b) sample calcinated for 9h.

### 3.2 Electrochemical Performance

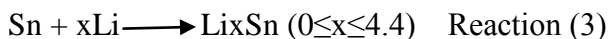
Fig. 3 presents typical charge–discharge voltage curves of the anodes constructed from SnO<sub>2</sub> nanoparticle at 0.2 C rate in the voltage range of 0.01 ~ 3.00 V (vs. Li/Li<sup>+</sup>). For clarity only selected cycles are shown. The theoretical discharge specific capacity of SnO<sub>2</sub> nanoparticle was 782 mAh g<sup>-1</sup>, while as shown in Fig. 3, the SnO<sub>2</sub> nanoparticle had high initial discharge specific capacity as approximate 1400~1600 mAh g<sup>-1</sup>. The initial discharge specific capacities of the as-prepared SnO<sub>2</sub> nanoparticle was much higher than the theoretical data. The extra capacity might result from the formation of SEI layer (solid electrolyte interface layer) which was known as a gel-like layer, containing ethylene oxide based oligomers, LiF, Li<sub>2</sub>CO<sub>3</sub>, and lithium alkyl carbonate (ROCO<sub>2</sub>Li), during the first discharging process[15, 16]. There was an discharge specific capacity attenuation during the next cycling. The discharge specific capacity of SnO<sub>2</sub> nanoparticle in the second cycle was about 1000 mAh g<sup>-1</sup>. After five cycling the discharge specific capacity fell to about 650~700 mAh g<sup>-1</sup>. In fact, after 15<sup>th</sup> cycling the discharge specific capacity continue fell down (not shown in Fig. 3). The discharge specific capacity attenuation might cause by the electrode pulverization and loss of interparticle contact or the particle with copper foil collector due to large volume expansion/contraction during repeated charging-discharging processes and severe particle aggregation. As reported for other metal oxide anode, Li storage in SnO<sub>2</sub> is primarily based on multiple electrochemical reactions of SnO<sub>2</sub> with Li. In discharge process, SnO<sub>2</sub> transformed to Sn, and Li<sup>+</sup> inserted into the anode to format Li<sub>2</sub>O. The reaction was as follow:



During the charge process, Sn can facilitate the decomposition of Li<sub>2</sub>O. The reaction of Li<sub>2</sub>O with Sn was as follow:



While during the first charge process, there is an extra reaction as follow:



According to the results here, SnO<sub>2</sub> nanoparticle can be an good candidate for anode application of lithium-ion battery, but the discharge specific capacity attenuation should be improved. To improve the stability of the discharge specific capacity, shell coating such as carbon coating, polypyrrole coating, polyaniline coating, is an effective strategy to improve the cycling stability. So in the future study, SnO<sub>2</sub> shell coating should be done to improve the cycling stability.

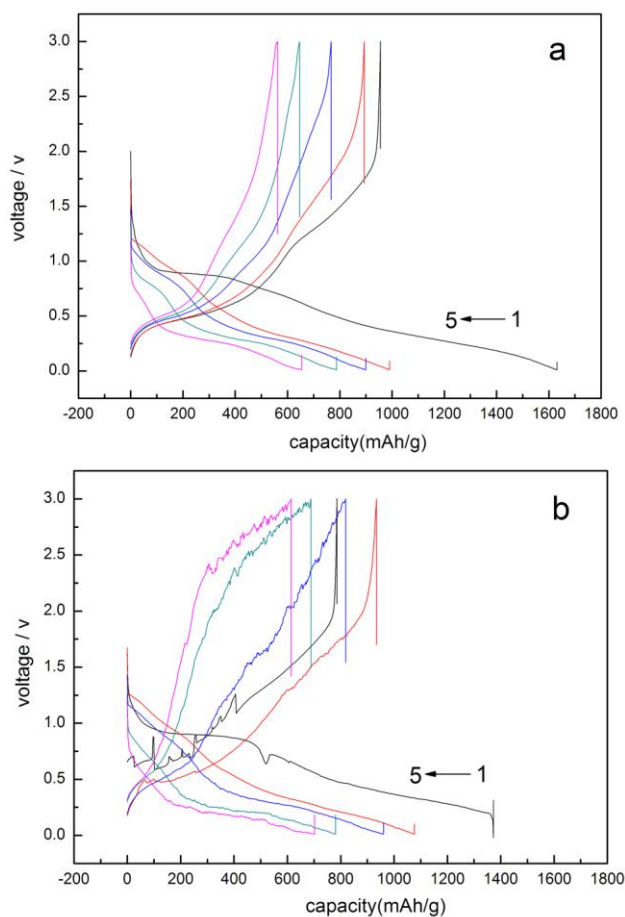


**Figure 3.** Charge-discharge curves for selected cycles for the as-prepared SnO<sub>2</sub> nanoparticle in the potential range of 0.01~3.00 V at 0.2 C. **(a)** sample calcinated for 7h , **(b)** sample calcinated for 9h.

In order to gain further understanding of the electrochemical performances, EIS testing were carried out. Fig. 4 presents the EIS results for lithium cells after the 5<sup>th</sup> cycle at open circuit voltage. The impedance spectra consist of an oblate semicircles in high-to-medium frequency region and a inclined line in low frequency region. An intercept at the Z<sub>real</sub> axis in high frequency region corresponds to the ohmic electrolyte resistance (R<sub>s</sub>). The semicircle in the high-to-medium frequency ascribes to the sum of the Li-ion migration resistance (R<sub>sf</sub>) through the SEI films and he charge

transfer resistance ( $R_{ct}$ ). The inclined line at low frequency region represents the warburg impedance ( $W_s$ ), which is associated with lithium-ion diffusion in the active material. In general, the ohmic electrolyte resistances of the as-prepared  $\text{SnO}_2$  nanoparticles are similar. The  $R_{sf}$  and  $R_{ct}$  value of the  $\text{SnO}_2$  nanoparticle calcinated for 9h is lower. The smaller the value of  $R_{sf}$  and  $R_{ct}$  is, the more favorable for the intercalation and deintercalation of lithium ion. So this indicates that the  $\text{SnO}_2$  nanoparticle calcinated for 9h is a little better.

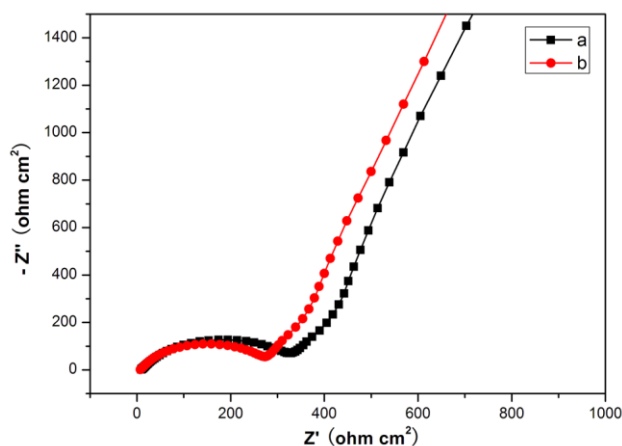


**Figure 4.** Nyquist plot obtained from Li/  $\text{SnO}_2$  cells after the 5<sup>th</sup> charge-discharge cycle at open circuit voltage. The frequency ranged from 0.1 Hz to 100 KHz with an applied AC signal amplitude of 5 mV. (a) sample calcinated for 7h , (b) sample calcinated for 9h.

#### 4. CONCLUSION

In summary,  $\text{SnO}_2$  nanoparticle is successfully prepared by the hydrolysis of  $\text{SnCl}_2$ . The  $\text{SnO}_2$  nanoparticle is cassiterite type which belongs to tetragonal crystal system with rutile structure. The results of galvanostatic cell cycling performances show that the  $\text{SnO}_2$  nanoparticle has high discharge specific capacity, but with relative low cycling stability. The sample calcinated for 9h has higher discharge specific capacity and lower electrochemical impedance.

#### ACKNOWLEDGEMENTS

This work was financially supported by Program for National Natural Scientific Fund (No.21463028), International Education Cooperation Base of Yunnan Minzu University (YMU 218-02001001002129), Innovative Research Team (in Science and Technology) in University of Yunnan Province (2010UY08, 2011UY09), Yunnan Provincial Innovation Team (2011HC008), the general program of the application and basic research foundation of Yunnan province (2013FZ080), the key project of scientific research foundation of educational bureau of Yunnan province (2013Z039), the scientific research foundation of educational bureau of Yunnan province (2013Y231), and the graduate program of scientific research foundation of educational bureau of Yunnan province (2013J120C).

## References

1. P. Poizot, S. Laruelle, S. Grugeon, L. Dupont, and J.M. Tarascon, *Nature*, 407 (2000) 496.
2. H.B. Wu, J.S. Chen, H.H. Hng, and X.W.D. Lou, *Nanoscale*, 4 (2012) 2526.
3. H. Wang, and A.L. Rogach, *Chem. Mater.*, 26 (2014) 123.
4. R. Demir-Cakan, Y.S. Hu, M. Antonietti, J. Maier, and M.M. Titirici, *Chem. Mater.*, 20 (2008) 1227.
5. M.S. Park, G.X. Wang, Y.M. Kang, D. Wexler, S.X. Dou, and H.K. Liu, *Angew. Chem. Int. Ed.*, 46 (2007) 750.
6. J. Wang, N. Du, H. Zhang, J. Yu, and D. Yang, *J. Phys. Chem. C*, 115 (2011) 11302.
7. M. Wang, Y. Gao, L. Dai, C. Cao, and X. Guo, *J. Solid State Chem.*, 189 (2012) 49.
8. C. Wang, G. Du, K. Ståh, H. Huang, Y. Zhong, and J.Z. Jiang, *J. Phys. Chem. C*, 116 (2012) 4000.
9. Y. Zhao, J. Li, N. Wang, C. Wu, G. Dong, and L. Guan, *J. Phys. Chem. C*, 116 (2012) 18612.
10. D. Wang, X. Li, J. Wang, J. Yang, D. Geng, R. Li, M. Cai, T.-K. Sham, and X. Sun, *J. Phys. Chem. C*, 116 (2012) 22149.
11. S.K. Park, S.H. Yu, N. Pinna, S. Woo, B. Jang, Y.H. Chung, Y.H. Cho, Y.E. Sung, and Y. Piao, *J. Mater. Chem.*, 22 (2012) 2520.
12. Q. Zhao, Y. Xie, T. Dong, and Z. Zhang, *J. Phys. Chem. C*, 111 (2007) 11598.
13. S. Han, B. Jang, T. Kim, S.M. Oh, and T. Hyeon, *Adv. Funct. Mater.*, 15 (2005) 1845.
14. C. Wang, Y. Zhou, M. Ge, X. Xu, Z. Zhang, and J.Z. Jiang, *J. Am. Chem. Soc.*, 132 (2010) 46.
15. J.Y. Xiang, J.P. Tu, L. Zhang, Y. Zhou, X.L. Wang, and S.J. Shi, *J. Power Sources*, 195 (2010) 313.
16. Z. Zhang, H. Chen, X. She, J. Sun, J. Teo, and F. Su, *J. Power Sources*, 217 (2012) 336.

© 2015 The Authors. Published by ESG ([www.electrochemsci.org](http://www.electrochemsci.org)). This article is an open access article distributed under the terms and conditions of the Creative Commons Attribution license (<http://creativecommons.org/licenses/by/4.0/>).